NACA RM E53J07

RESEARCH MEMORANDUM

MEASUREMENT OF HEAT-TRANSFER AND FRICTION COEFFICIENTS FOR FLOW OF AIR IN NONCIRCULAR DUCTS AT HIGH SURFACE TEMPERATURES

By Warren H. Lowdermilk, Walter F. Weiland, Jr.,
and John N. B. Livingood

Lewis Flight Propulsion Laboratory
Cleveland, Ohio

NATIONAL ADVISORY COMMITTEE
FOR AERONAUTICS

WASHINGTON
January 25, 1954

NACA RM E53J07

NATIONAL ADVISORY COMMITTEE FOR AERONAUTICS

RESEARCH MEMORANDUM

MEASUREMENT OF HEAT-TRANSFER AND FRICTION COEFFICIENTS FOR FLOW OF AIR IN NONCIRCULAR DUCTS AT HIGH SURFACE TEMPERATURES

By Warren H. Lowdermilk, Walter F. Weiland, Jr.,
and John N. B. Livingood

SUMMARY

Measurements of average heat-transfer and friction coefficients were obtained with air flowing through electrically heated ducts having square, rectangular (aspect ratio, 5), and triangular cross sections for a range of surface temperature from 540° to 1780° R and Reynolds number from 1000 to 330,000.

The results indicate that the effect of heat flux on correlations of the average heat-transfer and friction coefficients is similar to that obtained for circular tubes in a previous investigation and was nearly eliminated by evaluating the physical properties and density of the air at a film temperature halfway between the average surface and fluid bulk temperatures. With the Nusselt and Reynolds numbers based on the hydraulic diameter of the ducts, the data for the noncircular ducts could be represented by the same equations obtained in the previous investigation for circular tubes.

Correlation of the average difference between the surface corner and midwall temperatures for the square duct was in agreement with predicted values from a previous analysis. However, for the rectangular and triangular ducts, the measured corner temperature was greater by approximately 20 and 35 percent, respectively, than the values predicted by analysis.

INTRODUCTION

An experimental investigation was instituted at the NACA Lewis laboratory to obtain heat-transfer and related pressure-drop information for air flowing in tubes at high surface and fluid temperatures. The effects of such variables as surface temperature, inlet-air

temperature, length-to-diameter ratio, and tube-entrance configuration on heat transfer and pressure drop in smooth round tubes are summarized in reference 1.

The scope of the general investigation is extended herein to include the effect of flow-passage shape on heat-transfer and friction coefficients for air flowing through electrically heated square, triangular, and rectangular tubes at high heat-flux conditions. Data were obtained for a range of Reynolds number from 1000 to 330,000 and surface temperature from 540° to 1780° R, and the results are compared with those of reference 1 for circular tubes.

APPARATUS AND PROCEDURE

Arrangement of Apparatus

A schematic diagram of the heater tubes and associated equipment is shown in figure 1. The experimental setup is the same as described in reference 1. Compressed air is supplied through a pressure-regulating valve, a cleaner, and a surge tank to a second pressure-regulating valve where the flow rate is controlled. From this valve, the air flows through a bank of rotameters into a three-pass mixing tank, through the test section, and into a second mixing tank from which it is discharged to the atmosphere.

Electric power is supplied to the heater tube from a 208-volt, 60-cycle supply line through an autotransformer and a 14:1 power transformer. The low-voltage leads of the power transformer are connected to the heater-tube flanges by copper cables. The capacity of the electric equipment is 15 kilovolt-amperes.

Test Sections

Three different 24-inch-long cross-sectional shapes, as shown in figure 2 - square, equilateral triangle, and rectangle - were investigated, the inner dimensions of which were as follows:

Shape	Perimeter, in.	Hydraulic diam., in.	Length to hydraulic-diam. ratio
Square	1.80	0.45	53
Equilateral triangle	2.31	.45	53
Rectangle	3.0	.42	57

The test sections were fabricated from Inconel sheet stock with a thickness of 0.031 inch. The test-section sides were cut to the desired dimensions and clamped on ground-steel forms; each corner was welded with a heliarc welder. The excess weld material was ground off so that the corner wall thickness did not exceed 1/32 inch. The inner corners of the test sections were sharp and even along the entire length of the test section. Steel flanges welded to the test sections at each end provided electric contact with the transformer leads from the power supply. Channels were milled in the outer faces of the flanges to minimize end heat losses, and the test sections were thermally insulated.

Outside-wall temperatures were measured at 13 stations along the length of the test sections (fig. 2) with chromel-alumel thermocouples and a self-balancing indicating potentiometer. At each station, thermocouples were located at the center of each side, except for the rectangular test section, where the thermocouples were omitted on the short sides. Thermocouples were also located at each corner at the three stations located 3, 12, and 21 inches from the entrance.

Static-pressure taps were located 1/8 inch from the entrance and exit of each test section, and each section was fitted with a long-radius nozzle the throat dimensions of which matched the cross-sectional dimensions of the test section.

Range of Conditions

Heat-transfer and associated pressure-drop data were obtained with the square, the equilateral triangular, and the rectangular test sections with rounded entrances over a range of Reynolds number from 1000 to 330,000, average outside-wall temperatures from 540° to 1780° R, and heat-flux densities up to 120,000 Btu per hour per square foot of heat-transfer area.

SYMBOLS

The following symbols are used in this report:

A cross-sectional area, sq ft

c_p specific heat, Btu/(lb)(°F)

D inside hydraulic diameter, $\frac{4A}{\text{Perimeter}}$, ft

E voltage drop across test section, v

f	average friction coefficient
f_f	modified film friction coefficient
G	mass velocity, lb/(hr)(sq ft)
g	acceleration due to gravity, 4.17×10^8 ft/hr^2
h	average heat-transfer coefficient, Btu/(hr)(sq ft)($^\circ$F)
I	current flow through test section, amp
k	thermal conductivity, Btu/(hr)(sq ft)($^\circ$F/ft)
k^*	ratio of thermal conductivity of wall material to coolant
L	length of test section, ft
Nu	Nusselt number, hD/k
Pr	Prandtl number, $c_p\mu/k$
p	static pressure, lb/sq ft abs
Δp	over-all static-pressure drop across test section, lb/sq ft
Q_l	heat loss from test section to surroundings, Btu/hr
R	gas constant, 53.35 ft-lb/(lb)($^\circ$R)
Re	Reynolds number, $\rho VD/\mu$
S	heat-transfer area of test section, sq ft
s^*	ratio of wall thickness to hydraulic diameter
T	total temperature, $^\circ$R
T_b	average fluid bulk temperature, $\frac{T_1 + T_2}{2}$, $^\circ$R
T_f	average fluid film temperature, $\frac{T_s + T_b}{2}$, $^\circ$R
T_s	average surface temperature, $T_m + \frac{T_c - T_m}{2}$, $^\circ$R

t static temperature, °R

V velocity, ft/hr

W flow rate, lb/hr

γ ratio of specific heats

μ absolute viscosity, lb/(hr)(ft)

ρ density, lb/cu ft

Subscripts:

av average

b bulk (when applied to properties, indicates evaluation at average bulk temperature, T_b)

c peripheral location at corner of test section

f film (when applied to properties, indicates evaluation at average film temperature, T_f)

fr friction

m peripheral location midway between corners of test section

s surface (when applied to properties, indicates evaluation at average surface temperature, T_s)

1 test-section entrance

2 test-section exit

RESULTS AND DISCUSSION

Heat Balances

Heat balances for each test section are shown in figure 3, where the electric heat input minus the heat loss determined for condition of no air flow through the test section is plotted against the rate of heat transferred to the air as determined by air-flow rate and temperature measurements. The heat balances obtained at low heat inputs and correspondingly low flow rates were very poor. In this region the air temperature at the exit of the test section could not

be measured accurately, because the very low velocities in the outlet temperature mixing tank prevented the attainment of equilibrium conditions in the mixing tank.

The heat balances improved rapidly with increase in flow rate, and for values corresponding to turbulent flow in the test sections the data are in agreement with the match line (solid). The heat-transfer coefficients presented in reference 1 for round tubes, with which the present data are compared, were calculated from the flow rate and temperature rise of the air measurements; hence, for consistency the present data are calculated in a similar manner for flow rates corresponding to Reynolds numbers of 10,000 or greater. For lower flow rates, the electric heat-input and heat-loss measurements were believed to be more accurate than the measured outlet-air temperature. Therefore, the heat-transfer coefficients for Reynolds numbers less than 10,000 are calculated from the electric heat-input and heat-loss measurements.

Correlation of Heat-Transfer Coefficients

The average heat-transfer coefficient h was computed from the experimental data by the relation

$$h = \frac{Wc_{p,b}(T_2 - T_1)}{S(T_s - T_b)} \tag{1}$$

where

$$T_2 = T_1 + \frac{(3.415EI - Q_l)}{c_{p,b}}$$

for Reynolds numbers less than 10,000. The bulk temperature of the air T_b was taken as the arithmetic mean of the temperatures at the entrance T_1 and the exit T_2 of the test sections. The average surface temperature T_s was taken as the arithmetic mean of the average outside corner temperature and the average outside midwall temperature. The temperature drop through the wall was neglected.

The physical properties of air used in calculating the Nusselt, Reynolds, and Prandtl numbers are the same as those used in reference 1, wherein the viscosity and specific heat were based on values reported in reference 2, and the thermal conductivity was assumed to vary as the square root of temperature.

The results presented in reference 1 for turbulent flow in circular tubes indicate that the average Nusselt number decreases progressively

as the ratio of surface to fluid bulk temperature increases when the fluid properties are evaluated at the fluid bulk temperature. The effect of the ratio of surface to bulk temperature was eliminated by evaluating the properties of the air, including the density term in the Reynolds number at the film temperature, defined as the arithmetic average of the surface and bulk temperatures. The data for Reynolds numbers greater than 10,000 were well represented by the following relation:

$$\frac{hD}{k_f} = 0.034 \left(\frac{\rho_f V_b D}{\mu_f}\right)^{0.8} \left(\frac{c_{p,f}\mu_f}{k_f}\right)^{0.4} \left(\frac{L}{D}\right)^{-0.1}$$

which, for values of L/D between 53 and 57, becomes

$$\frac{hD}{k_f} = 0.023 \left(\frac{\rho_f V_b D}{\mu_f}\right)^{0.8} \left(\frac{c_{p,f}\mu_f}{k_f}\right)^{0.4} \tag{2}$$

The average heat-transfer coefficients obtained herein for square, rectangular, and triangular ducts for a range of Reynolds number from 1000 to 200,000 and ratios of surface to bulk temperature from 1.2 to 2.3 are correlated accordingly in figure 4. A solid line representing data obtained in reference 1 with a circular test section having a length-to-diameter ratio of 60 for similar conditions is included for comparison. For Reynolds numbers greater than 10,000, the reference line represents equation (2); for smaller Reynolds numbers the reference line represents the data of reference 1 recomputed on the basis of the electric heat-input and heat-loss measurements for purposes of comparison. The data for the square tube (fig. 4(a)) agree well with the reference line for all surface to bulk temperature ratios and Reynolds numbers. For the rectangular duct having an aspect ratio of 5, the data (fig. 4(b)) are considerably higher than the reference line for Reynolds numbers from 1000 to 10,000 and are represented by equation (2) for Reynolds numbers above 2500. The higher values are in agreement with data obtained for noncircular ducts at lower heat fluxes by other investigators. These data indicate that use of the hydraulic diameter does not result in correlation of data for various passage shapes in the laminar and transition flow regions. For Reynolds numbers above 40,000 the data fall slightly below the reference line.

In figure 4(c), the average heat-transfer coefficients for the triangular duct vary similarly to those obtained for the square duct. For Reynolds numbers above 10,000 the data were lower than the reference line by 5 to 15 percent and could best be represented by a line having a slope of 0.78 rather than 0.8. This difference in slope is also noticeable in figure 4(b) for the data of the rectangular duct for high Reynolds numbers. This variation in slope could be eliminated

by defining the average surface temperature as the midwall temperature instead of as the arithmetic average of the corner and midwall temperatures. For example (as is shown in fig. 7), the difference between the average surface and the average midwall temperatures for the triangular tube is 3 percent of the difference between the average midwall temperature and the fluid bulk temperature for a Reynolds number of 10,000, and 11 percent for a Reynolds number of 100,000. Evaluating the average heat-transfer coefficient on the basis of the difference between the midwall and fluid bulk temperatures would result in a corresponding increase in the average heat-transfer coefficient and, hence, would bring the data into agreement with the reference line for circular tubes. Measurements of the variation in rate of heat transfer around the periphery of noncircular ducts are required in order to define the average surface temperature for evaluating the average heat-transfer coefficient.

Correlation of Friction Coefficients

The method of calculating the average friction coefficient is essentially the same as described in reference 1, wherein

$$f_f = \frac{\Delta p_{fr}}{4 \frac{L}{D} \frac{\rho_f V_b^2}{2g}} \tag{3}$$

where

$$\Delta p_{fr} = (p_1 - p_2) - \frac{G^2 R}{g} \left(\frac{t_2}{p_2} - \frac{t_1}{p_1} \right)$$

$$\rho_f = \left(\frac{\rho_1 + \rho_2}{2} \right) \left(\frac{t_b}{t_f} \right)$$

and

$$t = - \frac{\gamma g}{(\gamma - 1) R} \left(\frac{p}{G} \right)^2 + \sqrt{\left[\frac{\gamma g}{(\gamma - 1) R} \left(\frac{p}{G} \right)^2 \right]^2 + 2T \frac{\gamma g}{(\gamma - 1) R} \left(\frac{p}{G} \right)^2}$$

The subscripts 1 and 2 refer to positions within the ducts, located 1/8 inch from the entrance and exit ends of the ducts, respectively. For Reynolds numbers less than 10,000 the exit static temperature t_2 is based on the value of the exit total temperature T_2 determined from the electric heat-input and heat-loss measurements, as was mentioned in the preceding section.

The average friction coefficients as calculated above are shown in figure 5 correlated by the method summarized in reference 1 for high heat-flux conditions. Included for comparison is the line representing the Kármán-Nikuradse relation for turbulent flow in pipes modified for the effect of heat flux on the friction coefficient, which is

$$\frac{1}{\sqrt{8\,\frac{f_f}{2}}} = 2\log_{10}\left(\frac{\rho_f V_b D}{\mu_f}\sqrt{8\,\frac{f_f}{2}}\right) - 0.8 \qquad (4)$$

In figure 5(a), the average friction coefficients for the square duct for Reynolds numbers above 10,000 to 20,000 agree reasonably well with the reference line for circular tubes, although the friction coefficient increases with an increase in heat flux or surface to fluid bulk temperature ratio. In the transition region for low Reynolds numbers, the friction coefficient varies considerably with heat flux. Similar variations were obtained in reference 1 for circular tubes.

The data for the rectangular and triangular ducts (figs. 5(b) and (c), respectively) indicate that the friction coefficient increases more with increasing heat flux than in the square duct (fig. 5(a)), which may possibly be caused by the development of secondary flows in the rectangular and triangular ducts.

Correlation of Peripheral Temperature Variations

Corner surface temperatures were measured at three stations along the length of each test section (3, 12, and 21 in. from entrance). The average differences between the corner and midwall temperatures are plotted against the mass velocity in figure 6. The average difference plotted herein was taken as the arithmetic average of the differences between the local average corner and midwall temperatures at each station. In general, the local average peripheral temperature difference increased along the length of the test section; however, in several instances the local values near the exit were less than those measured at the center station, which indicates the possibility of locally developed secondary flow near the corners. The average peripheral temperature differences increased at a decreasing rate with increases in mass velocity and heat flux. Maximum values of 35°, 127°, and 110° R were obtained for the square, the rectangular, and the triangular ducts, respectively.

In reference 3, a method was developed for predicting peripheral wall-temperature variations for flow in noncircular-tube heat exchangers with internal heat generation in the tube walls based on shear-stress

distributions measured by Nikuradse for flow in noncircular ducts. The average peripheral temperature differences are correlated accordingly in figure 7, where the ratio of the difference between the corner and the midwall temperatures to the difference between the surface (which was taken as the average midwall temperature) and fluid bulk temperatures is plotted against the dimensionless parameter, Nusselt number divided by the ratio of wall thickness to hydraulic diameter of the flow passage and the ratio of thermal conductivity of the wall material to the fluid (wherein the average heat-transfer coefficient is based on the difference between the average midwall and fluid bulk temperature). Included for comparison are the reference lines calculated for turbulent flow in the ducts from reference 3 for the case of no flow over the outer surface of the duct; hence for the heat-transfer coefficient for the outer surface equal to zero. The data for the square duct agree fairly well with the predicted values in the turbulent-flow range. The measured values for the rectangular and triangular ducts were greater on the average by about 20 and 35 percent, respectively, than the predicted values. This difference in measured and predicted values results in part from the assumption of similarity between variation of rate of heat-transfer and shear-stress distribution around the periphery of a noncircular duct and in part from the uncertainty in estimating the shear-stress distribution for a duct with aspect ratio of 5 from measurements obtained for a duct with aspect ratio of 3.5. Similar results are indicated for the triangular duct. Maximum values of the ratio of the average difference between the corner and midwall temperatures to the difference between the average surface and bulk temperatures obtained were 0.05, 0.25, and 0.20 for the square, the rectangular, and the triangular ducts, respectively.

2-86

SUMMARY OF RESULTS

The results of this investigation of heat transfer and pressure drop for air flowing through noncircular ducts having square, rectangular (aspect ratio, 5), and equilateral triangular cross sections for a range of surface temperature from 540° to 1780° R, corresponding surface to bulk temperature ratio from 1.2 to 2.3, and Reynolds numbers from 1000 to 330,000 may be summarized as follows:

1. The effect of the ratio of surface to bulk temperature on correlations of the average heat-transfer and friction coefficients was the same as that obtained in a previous investigation for similar ranges of conditions for flow in circular tubes and was nearly eliminated by evaluating the physical properties and density of the air at a film temperature halfway between the bulk and surface temperatures.

2. Correlations of the average heat-transfer and friction coefficients were in reasonable agreement with the results obtained for the circular tubes with the Nusselt number and Reynolds number based on the hydraulic diameter of the duct.

3. Correlation of the average peripheral temperature difference for the square duct was in agreement with values predicted by a previous analysis. However, the measured values for the rectangular and triangular ducts were greater by approximately 20 and 35 percent, respectively, than the predicted values.

4. Maximum values of the ratio of the average difference between the corner and midwall temperatures to the difference between the average surface and bulk temperatures obtained were 0.05, 0.25, and 0.20 for the square, the rectangular, and the triangular ducts, respectively.

Lewis Flight Propulsion Laboratory
National Advisory Committee for Aeronautics
Cleveland, Ohio, October 9, 1953

REFERENCES

1. Humble, Leroy V., Lowdermilk, Warren H., and Desmon, Leland G.: Measurements of Average Heat-Transfer and Friction Coefficients for Subsonic Flow of Air in Smooth Tubes at High Surface and Fluid Temperatures. NACA Rep. 1020, 1951. (Supersedes NACA RM's E7L31, E8L03, E50E23, and E50H23.)

2. Keenan, Joseph H., and Kaye, Joseph: Thermodynamic Properties of Air. John Wiley & Sons, Inc., 1945.

3. Eckert, E. R. G., and Low, George M.: Temperature Distribution in Internally Heated Walls of Heat Exchangers Composed of Noncircular Flow Passages. NACA RM E50J25, 1950.

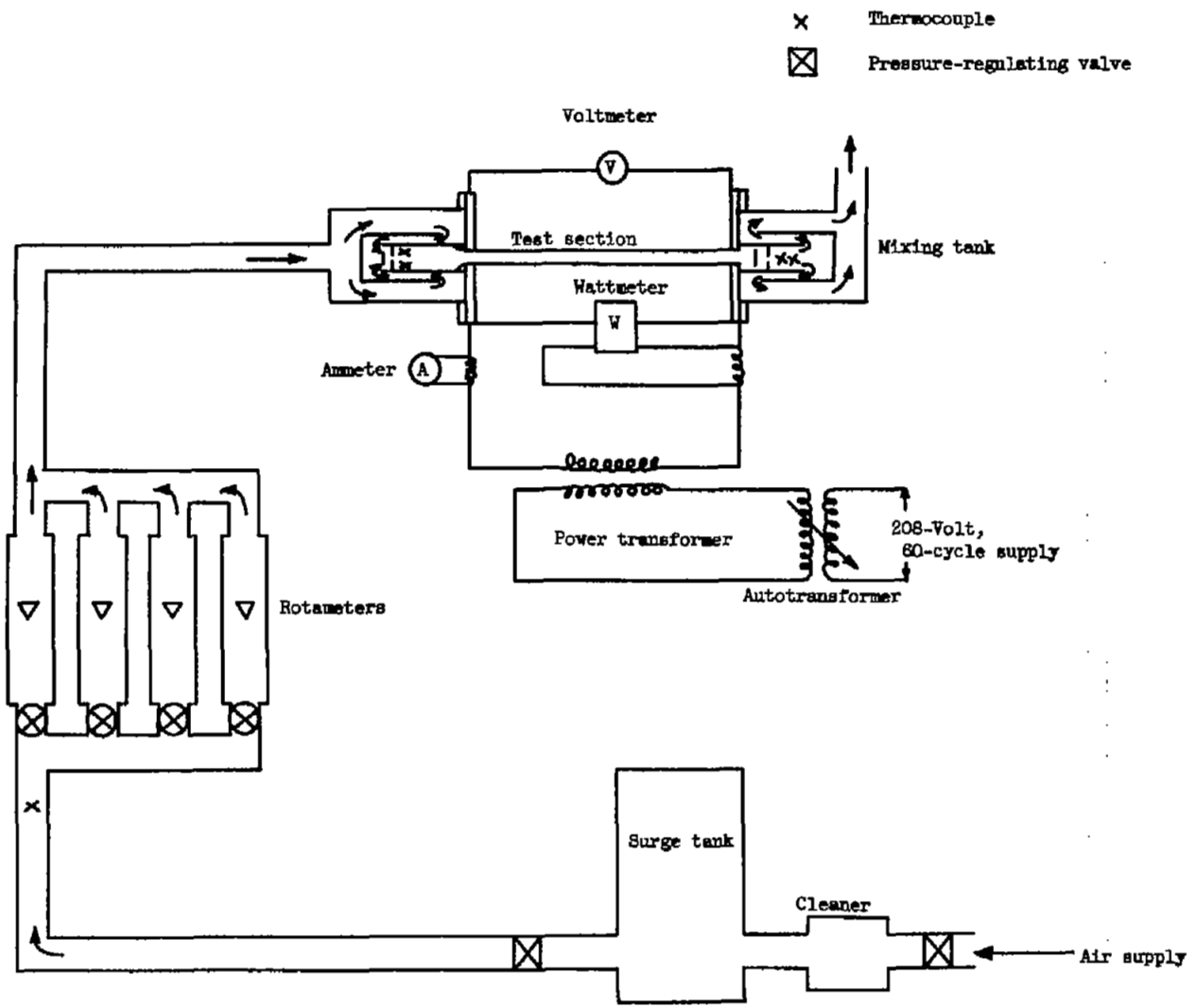

Figure 1. - Schematic diagram showing arrangement of apparatus.

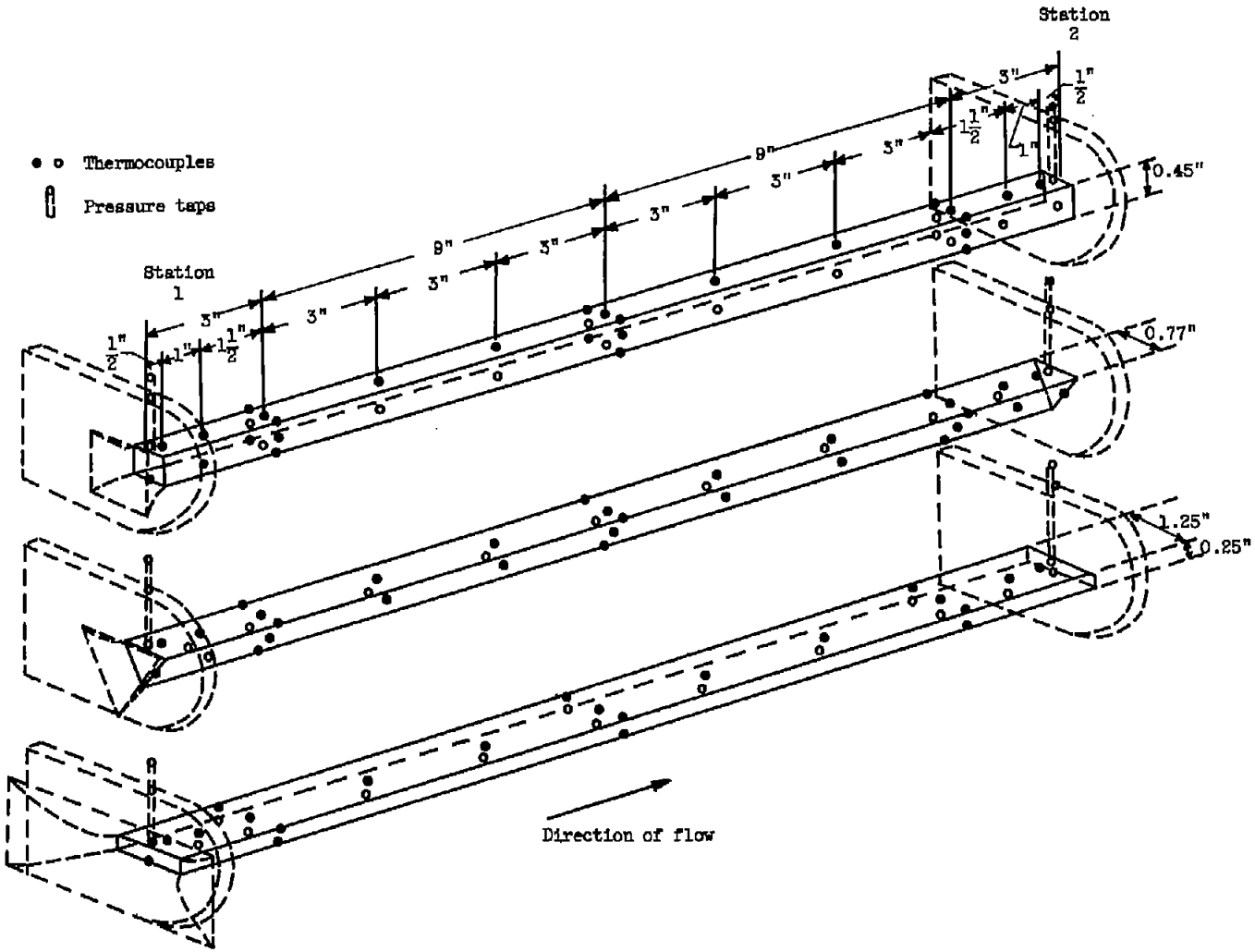

Figure 2. - Test sections showing thermocouple and pressure-tap locations.

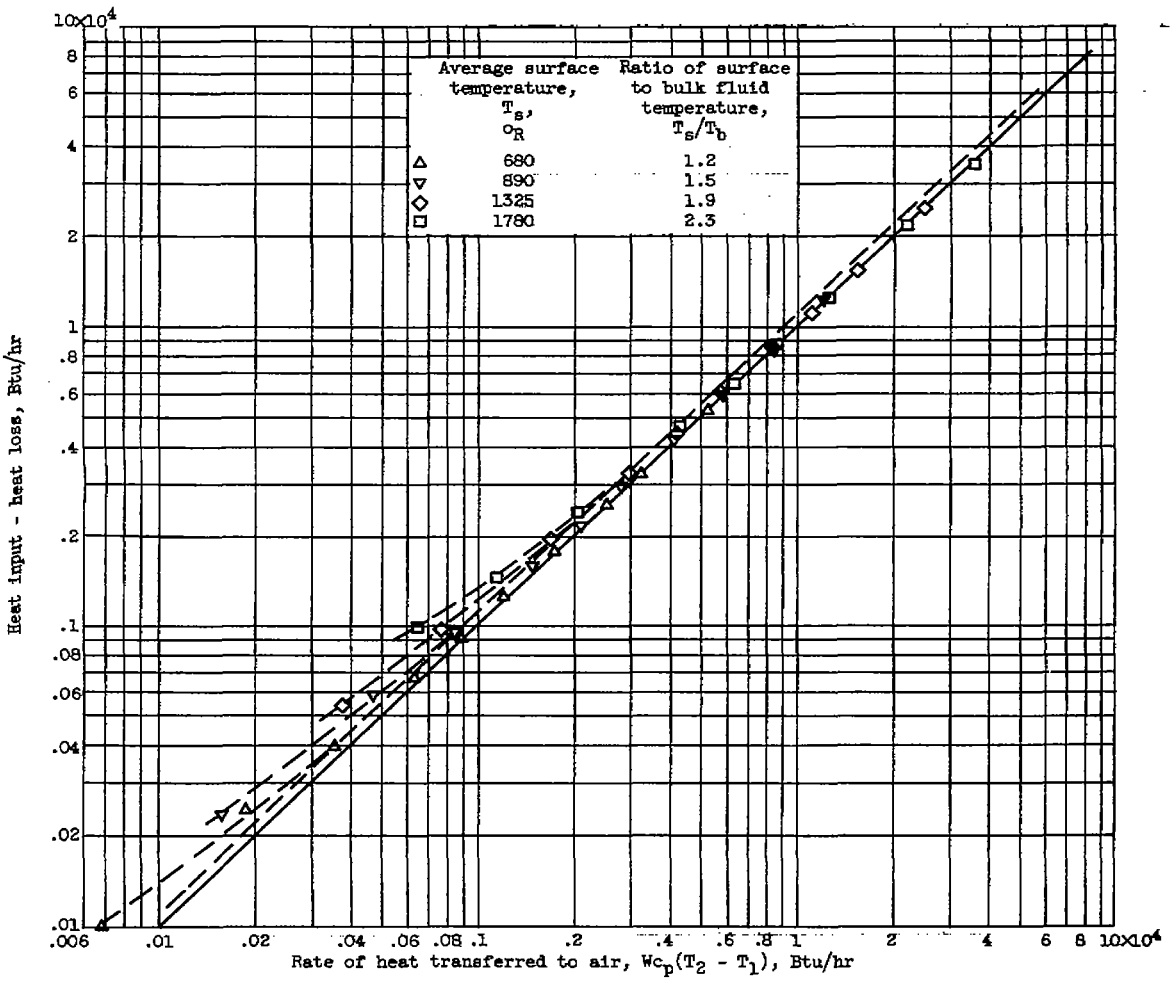

(a) Square duct.

Figure 3. - Heat balance.

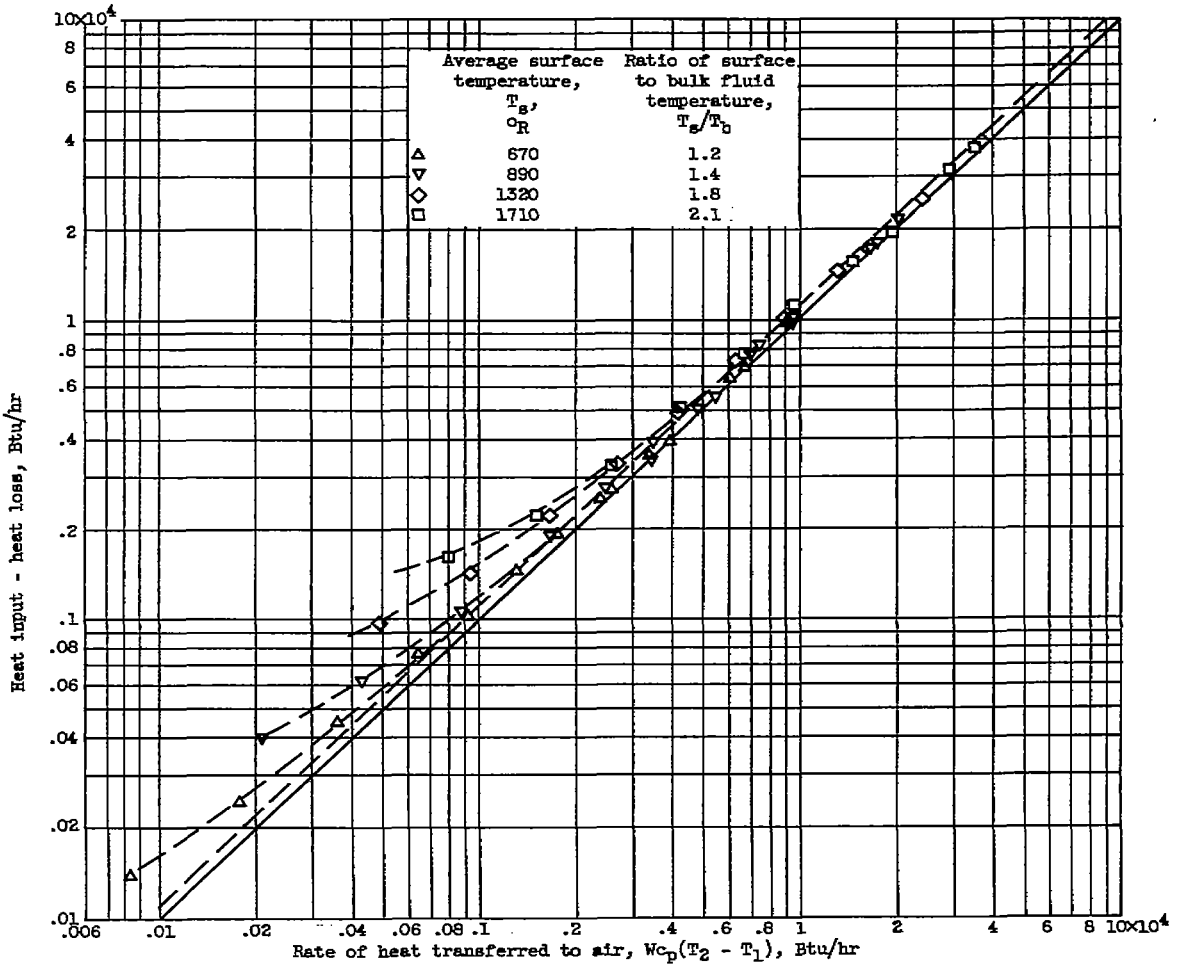

(b) Rectangular duct.

Figure 3. - Continued. Heat balance.

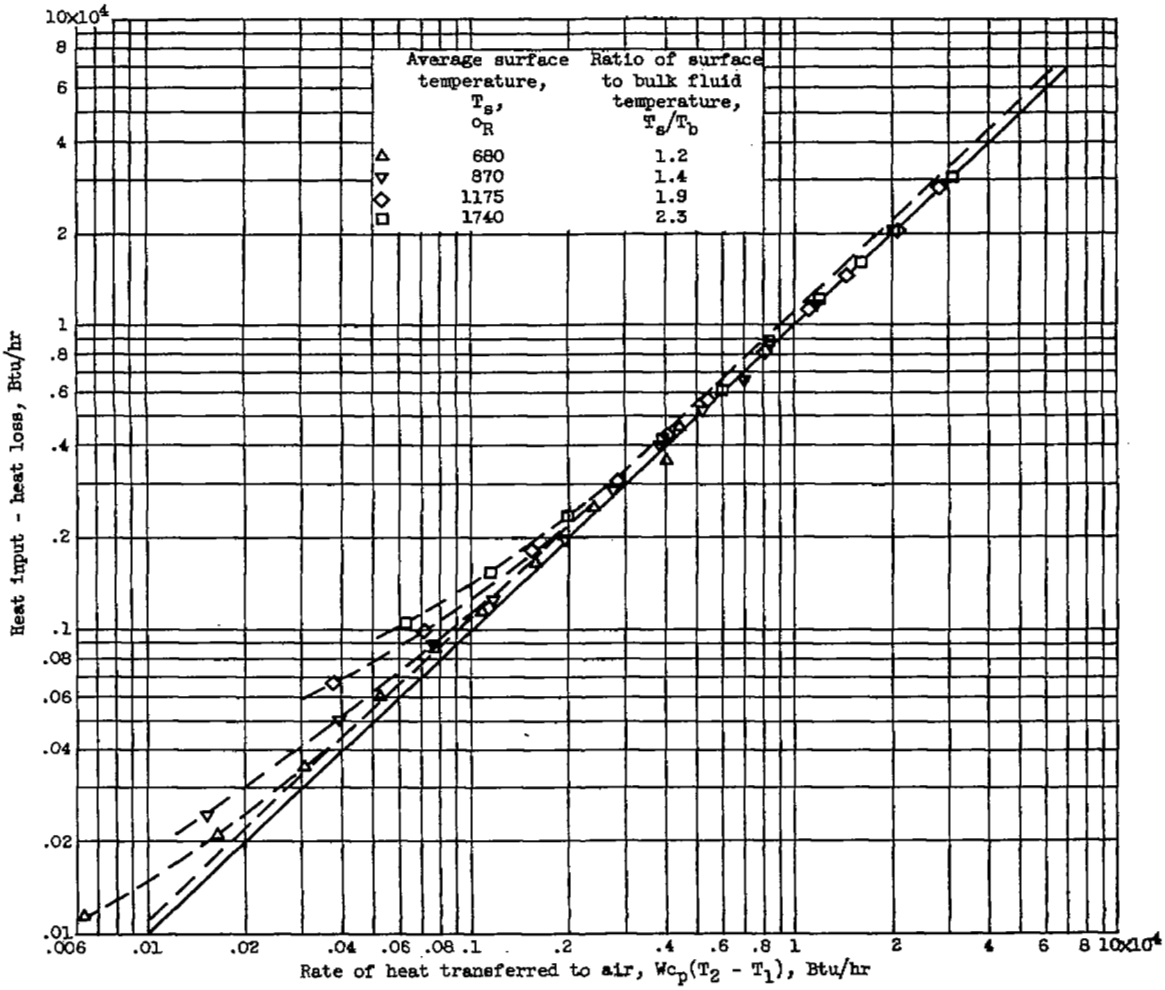

(c) Triangular duct.

Figure 3. - Concluded. Heat balance.

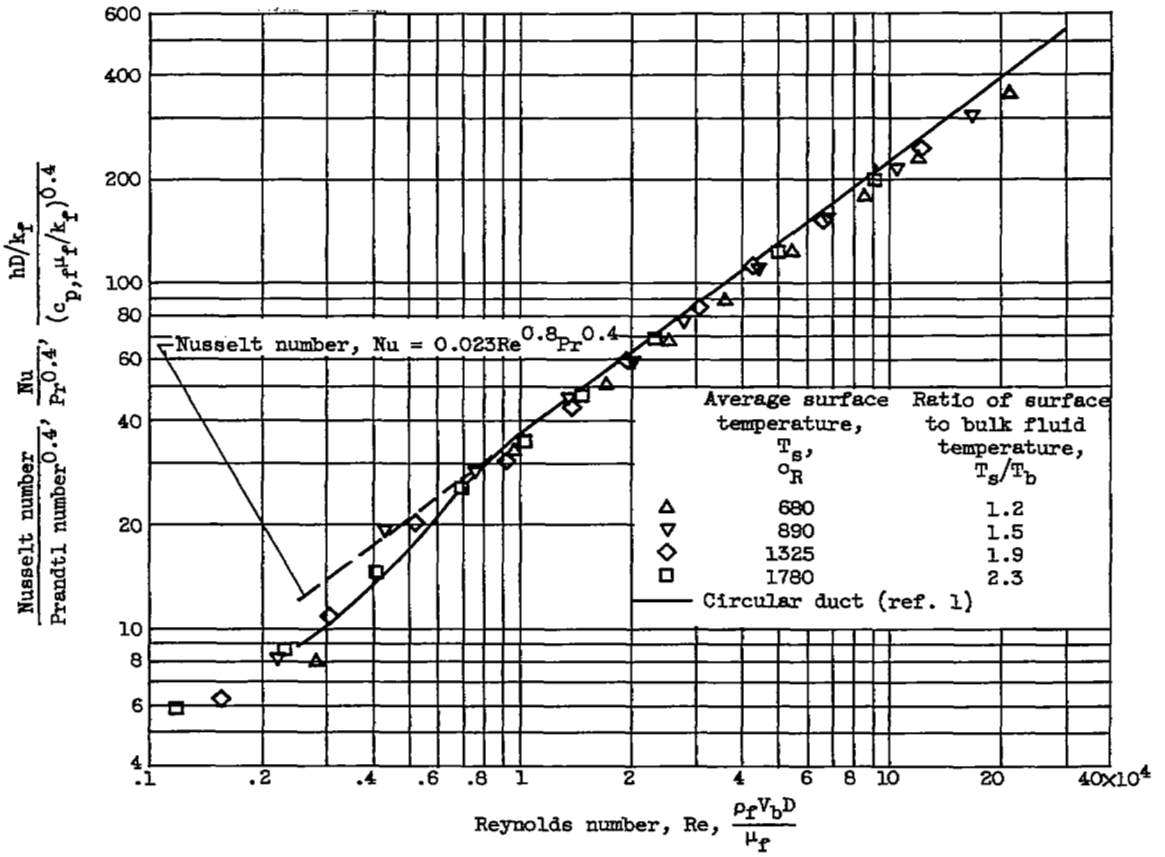

(a) Square duct.

Figure 4. - Correlation of heat-transfer coefficients for air flow in ducts with variable heat flux. Bellmouth entrance; inlet temperature, 535° R; properties of air evaluated at film temperature.

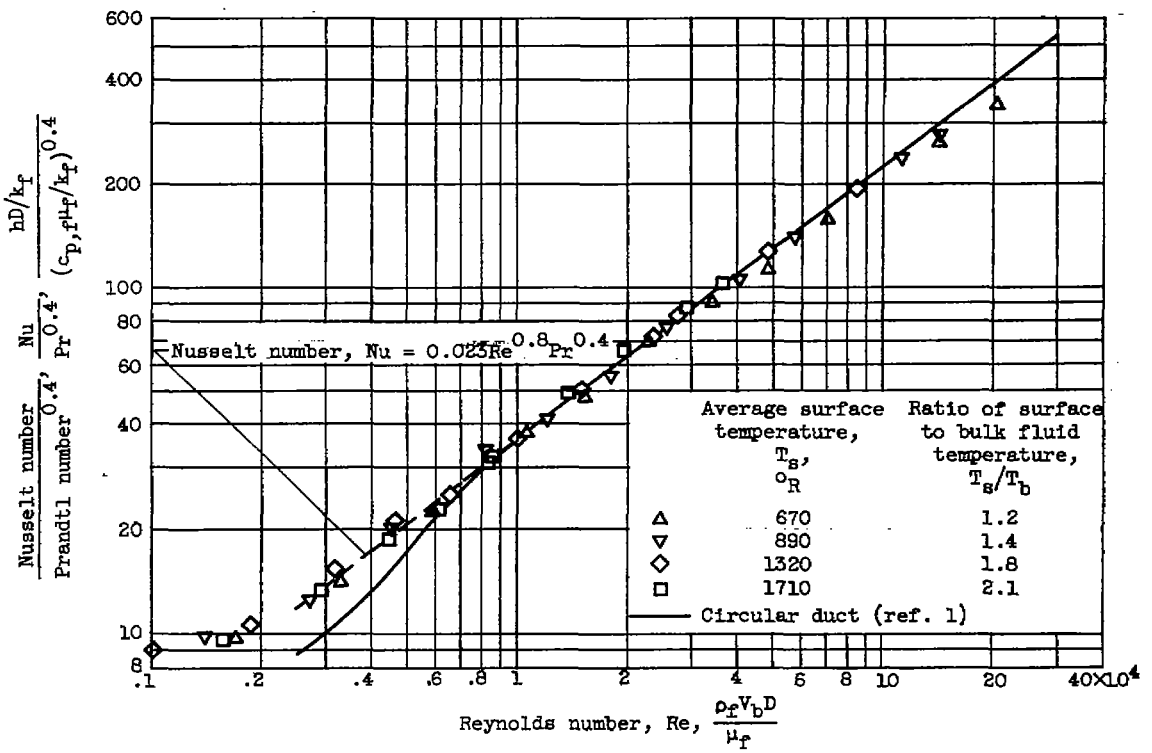

(b) Rectangular duct.

Figure 4. - Continued. Correlation of heat-transfer coefficients for air flow in ducts with variable heat flux. Bellmouth entrance; inlet temperature, 535° R; properties of air evaluated at film temperature.

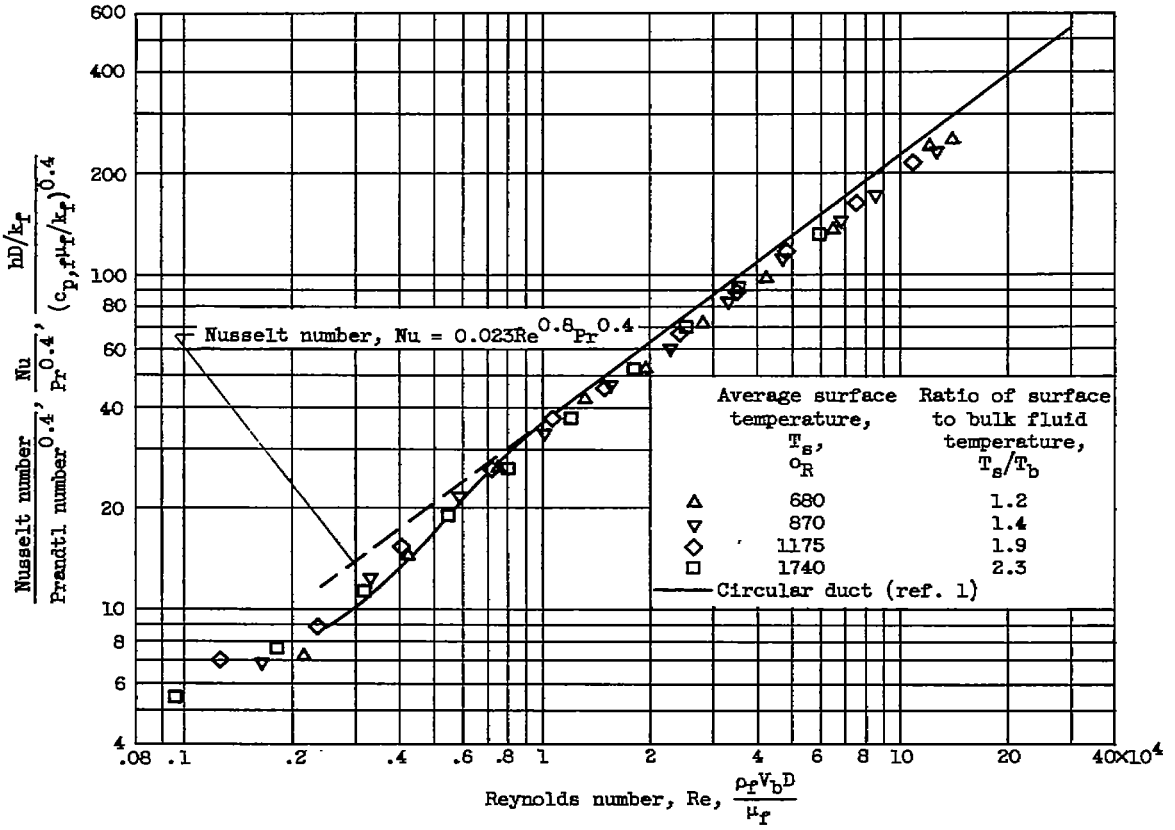

(c) Triangular duct.

Figure 4. - Concluded. Correlation of heat-transfer coefficients for air flow in ducts with variable heat flux. Bellmouth entrance; inlet temperature, 535° R; properties of air evaluated at film temperature.

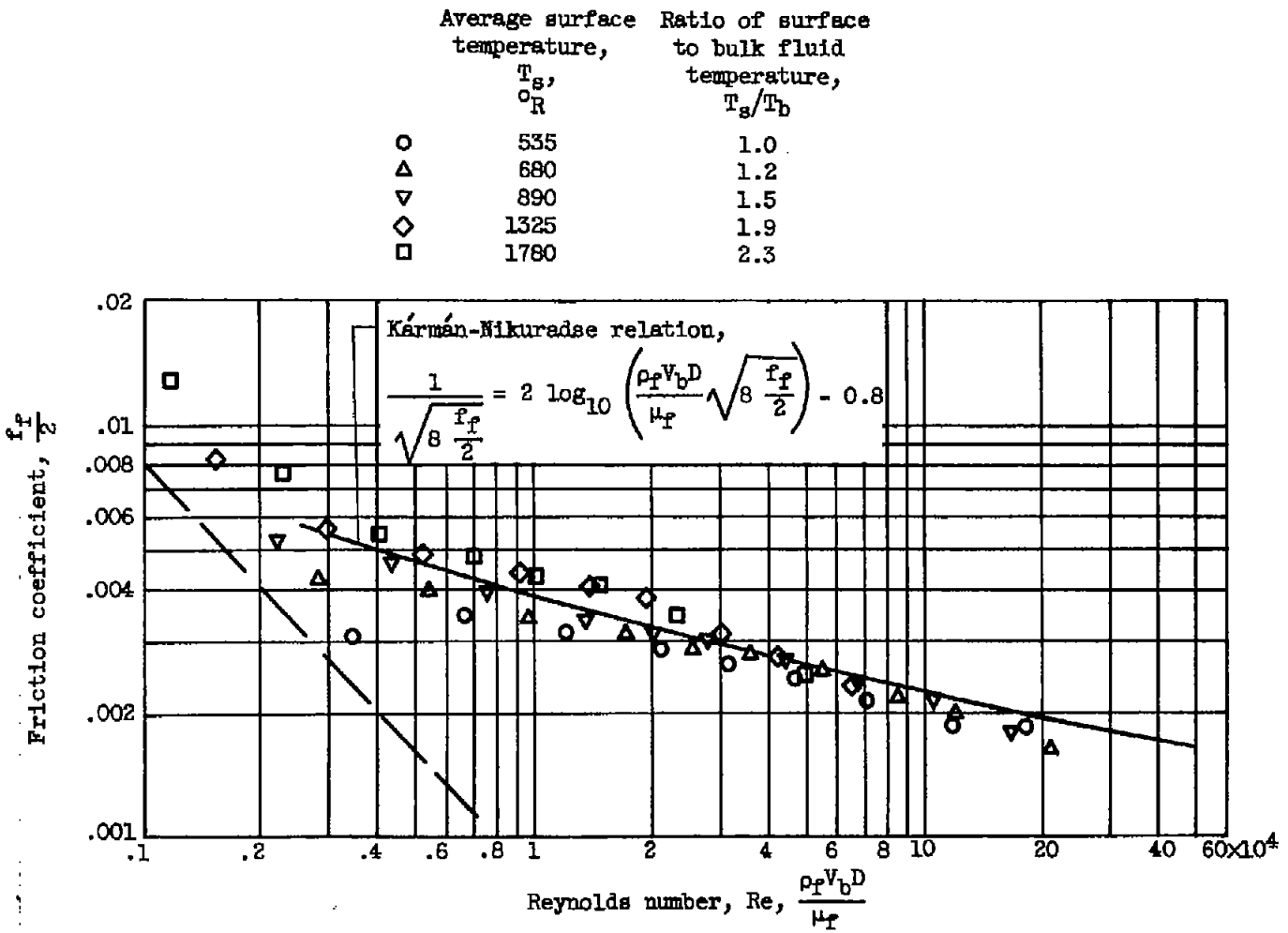

(a) Square duct.

Figure 5. - Correlation of friction coefficients for air flow in ducts with variable heat flux. Viscosity and density evaluated at film temperature.

	Average surface temperature, T_s, °R	Ratio of surface to bulk fluid temperature, T_s/T_b
○	535	1.0
△	670	1.2
▽	890	1.4
◇	1320	1.8
□	1710	2.1

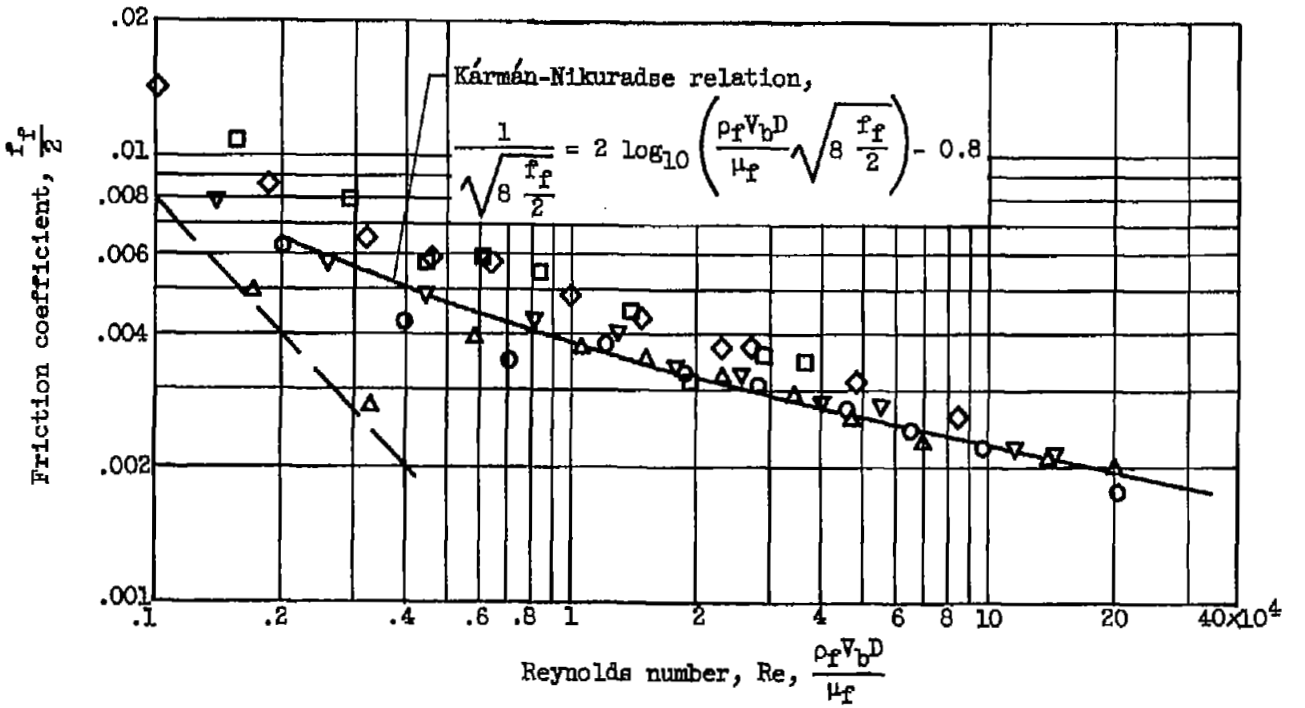

(b) Rectangular duct.

Figure 5. - Continued. Correlation of friction coefficients for air flow in ducts with variable heat flux. Viscosity and density evaluated at film temperature.

	Average surface temperature, T_s, °R	Ratio of surface to bulk fluid temperature, T_s/T_b
○	535	1.0
△	680	1.2
▽	870	1.4
◇	1175	1.9
□	1740	2.3

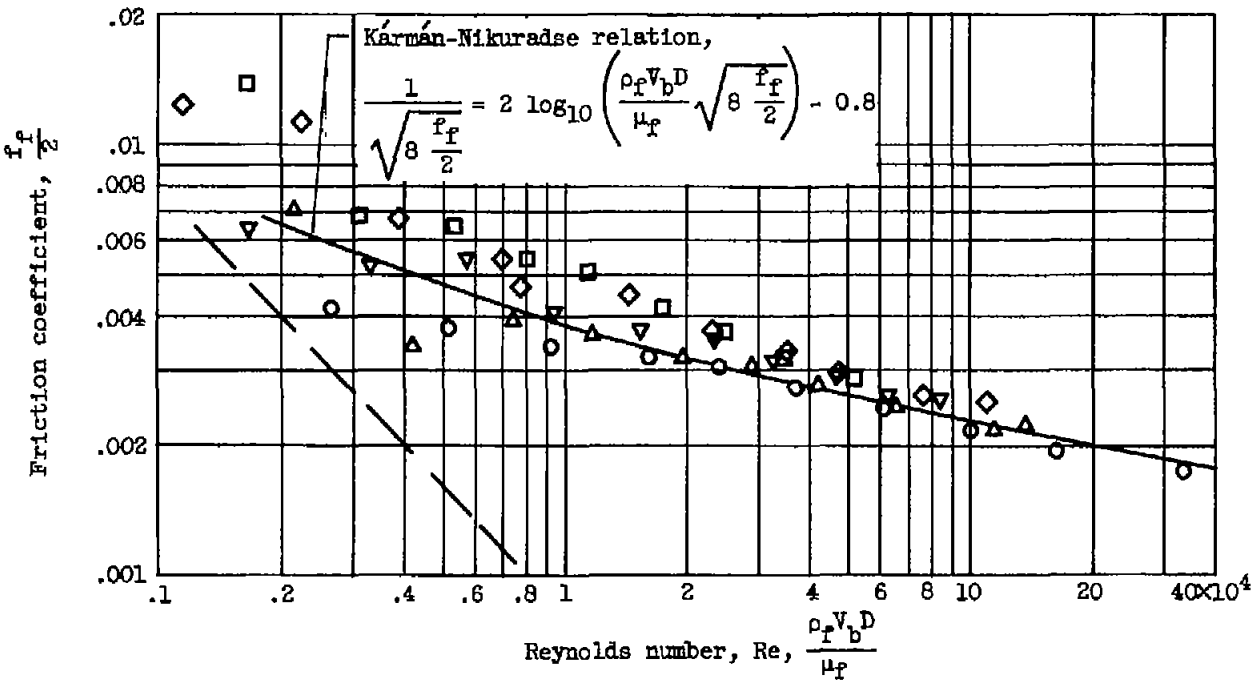

(c) Triangular duct.

Figure 5. - Concluded. Correlation of friction coefficients for air flow in ducts with variable heat flux. Viscosity and density evaluated at film temperature.

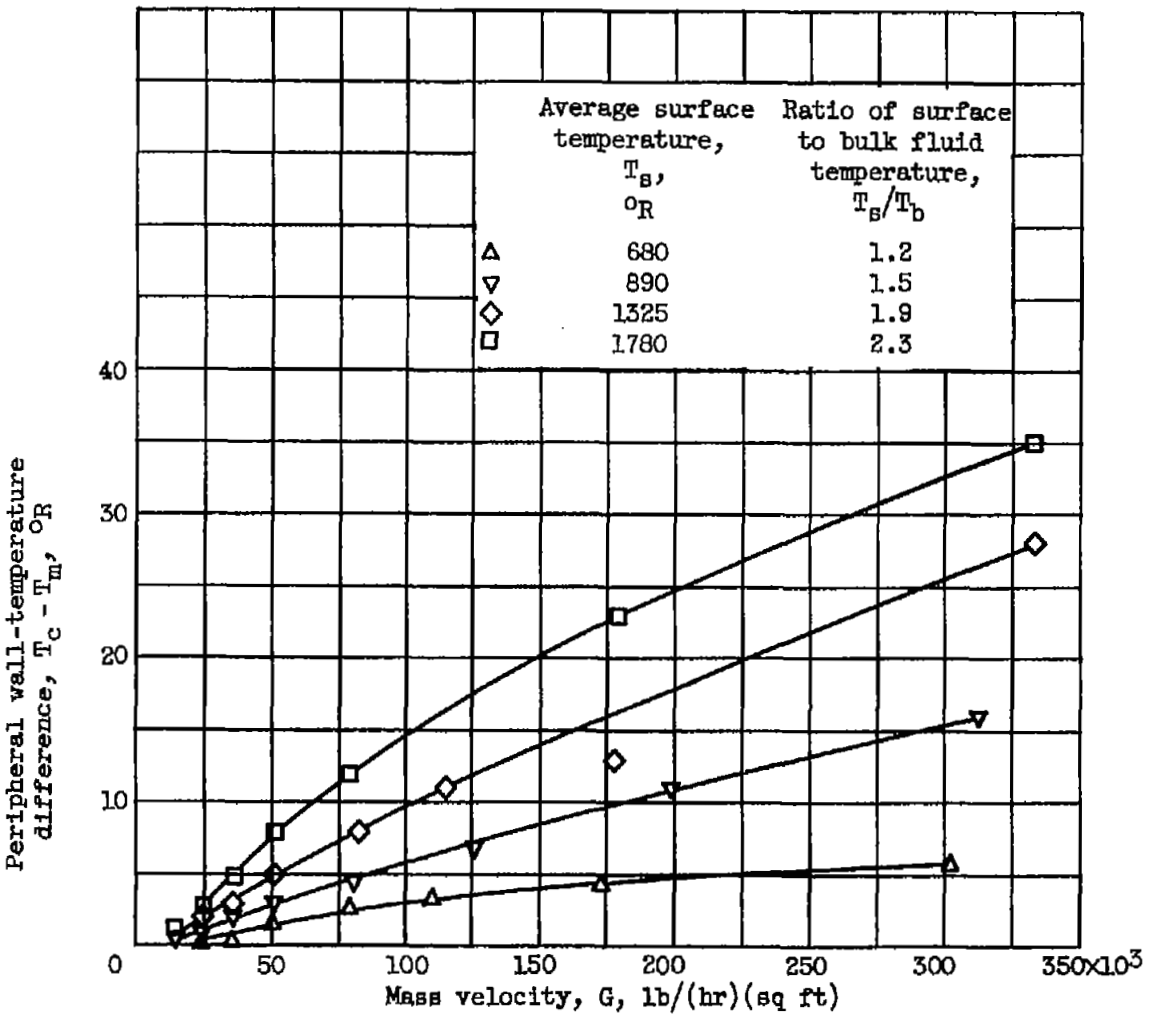

(a) Square duct.

Figure 6. - Variation of peripheral wall-temperature difference with mass velocity at various average wall temperatures.

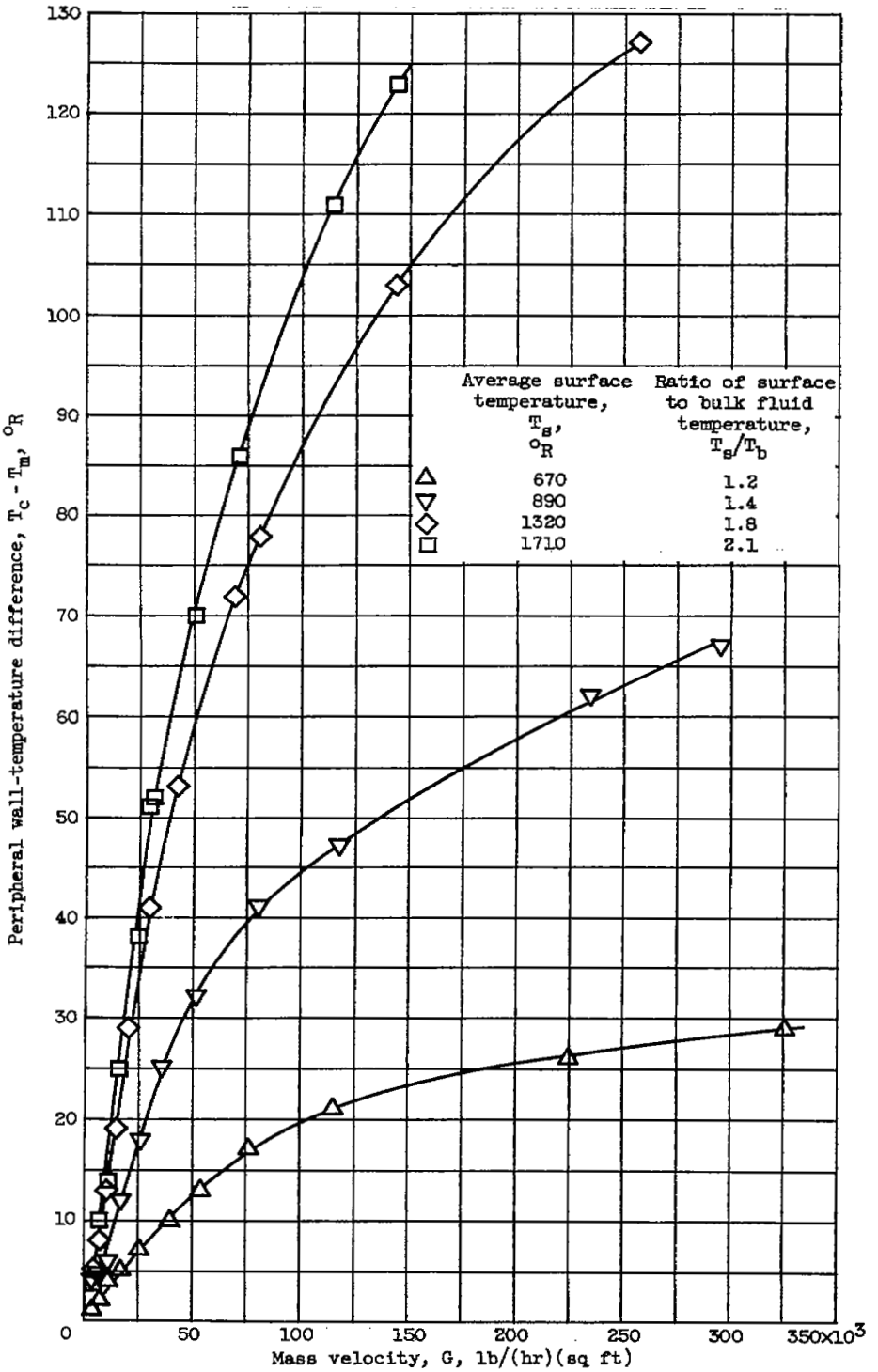

(b) Rectangular duct.

Figure 6. - Continued. Variation of peripheral wall-temperature difference with mass velocity at various average wall temperatures.

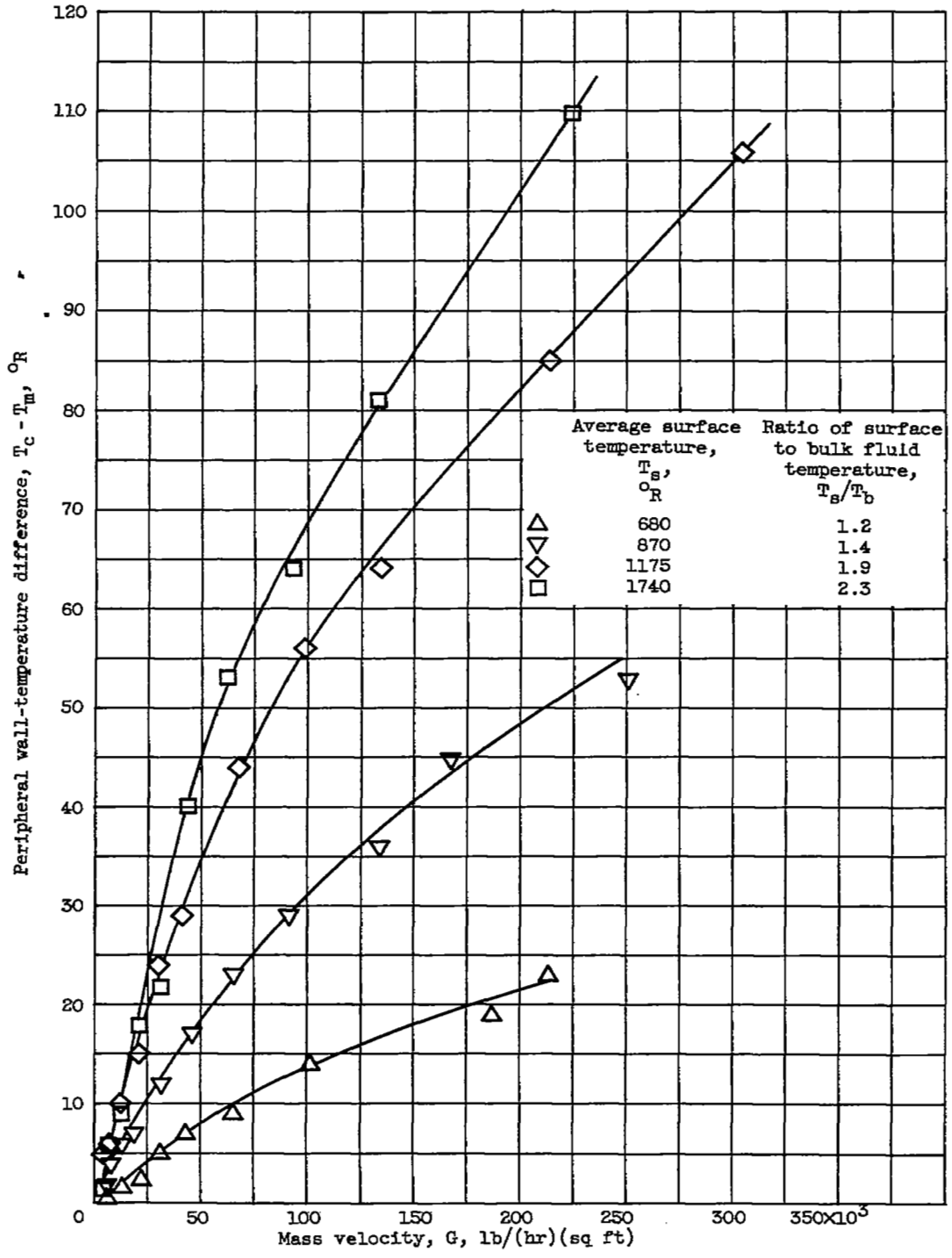

(c) Triangular duct.

Figure 6. - Concluded. Variation of peripheral wall-temperature difference with mass velocity at various average wall temperatures.

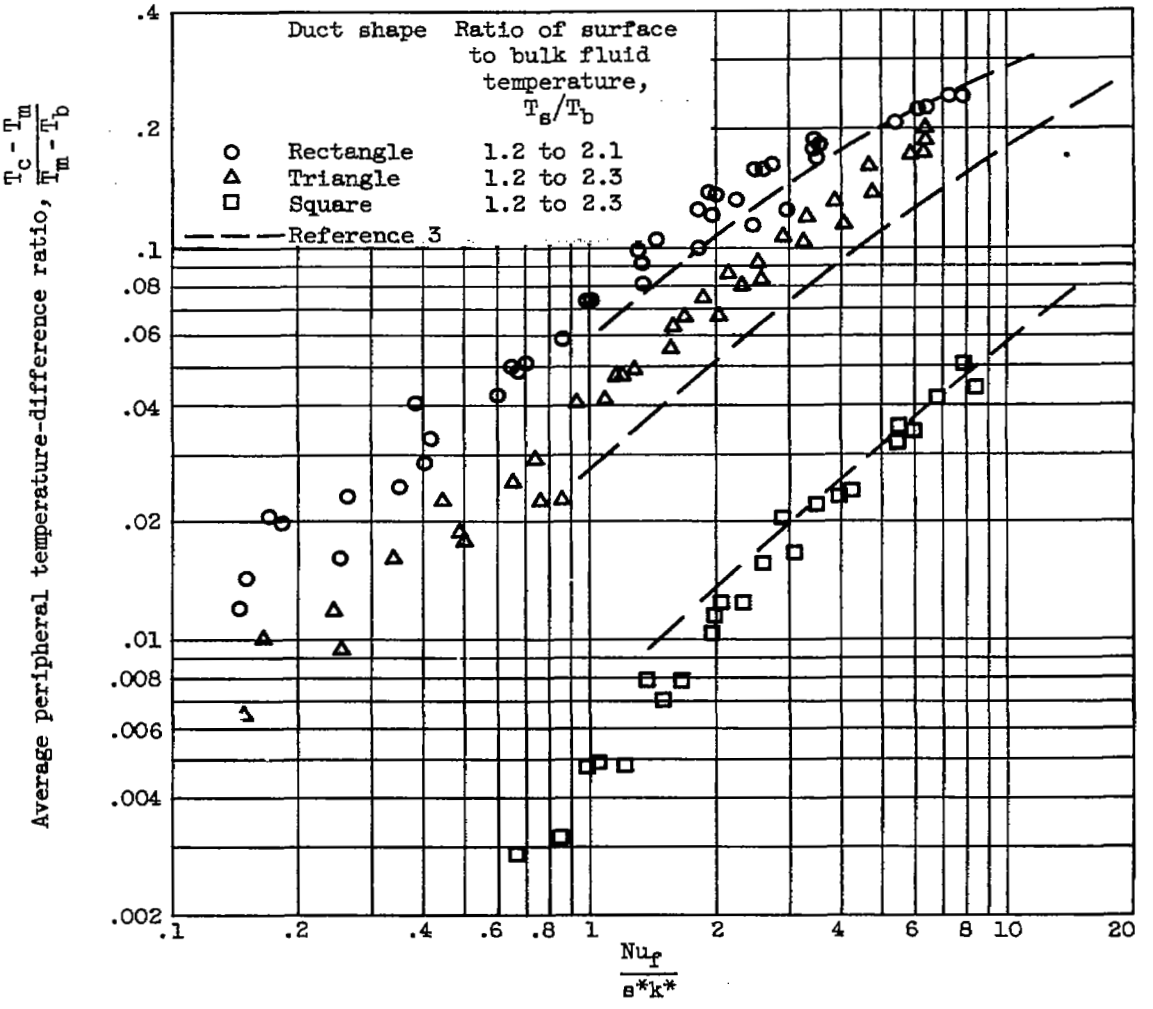

Figure 7. - Correlation of average peripheral temperature difference for flow in noncircular ducts with variable heat flux.

NACA-Langley - 1-25-54 - 325